ELSEVIER

Journal of Organometallic Chemistry 637–639 (2001) 311–317

Journal of Organometallic Chemistry

www.elsevier.com/locate/jorganchem

Electrostatic field effects manifested in ferrocenyl metal complexes and the crystal structure of $[Fe(\eta^5\text{-}C_5H_5)(\eta^5\text{-}C_5H_4CH{=}NNHC_5H_4N)]\cdot HCl$

Jack Silver [a,*], George R. Fern [a], John R. Miller [a], Elizabeth Slade [b], Mustafa Ahmet [b], Andrew Houlton [b,1], David J. Evans [c], G. Jeffery Leigh [d]

[a] *School of Chemical and Life Sciences, University of Greenwich, Woolwich Campus, Wellington Street, Woolwich, London SE18 6PF, UK*
[b] *Department of Chemical and Biological Sciences, Central Campus, University of Essex, Wivenhoe Park, Colchester CO4 3SQ, UK*
[c] *Department of Biological Chemistry, John Innes Centre, Norwich Research Park, Colney, Norwich NR4 7UH, UK*
[d] *School of Chemistry, Physics and Environmental Science, The University of Sussex, Falmer, Brighton, East Sussex BN1 9QJ, UK*

Received 4 January 2001; received in revised form 8 March 2001; accepted 13 March 2001

Abstract

The structure of $[Fe(\eta^5\text{-}C_5H_5)(\eta^5\text{-}C_5H_4CH{=}NNHC_5H_4N)]\cdot HCl$ (**1**·HCl) has been solved to $R = 0.05$ and is described. The parent compound has been shown to act as a ligand for a range of M^{2+} cations in the form $\mathbf{1}MCl_2$ (where $M = Cd^{2+}$, Cu^{2+}, Zn^{2+}, Sn^{2+}, Pd^{2+} and Fe^{2+}). ^{57}Fe Mössbauer spectroscopy has been used to probe the ferrocenyl iron electronic environments to give a ligand's eye view of the metal bonding. Two compounds of the formula $[\mathbf{1}M(H_2O)_4][PF_6]_2$ where $M = Fe^{2+}$ or Zn^{2+} were also prepared. The ferrocenyl quadrupole splittings of these two compounds were much smaller than those of the corresponding chloride. The change is explained in terms of the electric field experienced by the ferrocenyl iron atoms. In the chloride complexes the field from the M^{2+} is compensated by the chloride anions, whereas in the two $[PF_6]^-$ salts the charge on the M^{2+} is not compensated in the first coordination sphere. The ferrocenyl iron is thus directly exposed to the M^{2+} charge and it is the effect of this that gives rise to the small quadrupole splitting value. This is the first time such a field effect has been observed on a ferrocenyl iron by Mössbauer spectroscopy. The coordination geometry of the inorganic iron(II) environment is also elucidated as tetrahedral in $\mathbf{1}MCl_2$ and distorted octahedral in $[LM(H_2O)_4][PF_6]_2$.

Keywords: Ferrocene; Mössbauer

1. Introduction

There has been much interest in metal–metal interactions in ferrocene complexes in the last 15 years [1–8]. In addition to its interesting substitution chemistry, ferrocene can also act as a one electron donor undergoing oxidation to the ferrocenium ion. This has led to the use of ferrocene as a model for sensors and non-linear optical materials [9,10]. The interaction of different metals with the iron of the ferrocene moiety [10], and their effect on the ferrocene electronic environment can be probed by Mössbauer spectroscopy. In this work derivatised ferrocene carbaldehyde was used as a ligand substituent to give a ligand's eye view of such interactions. On adding an electron donating substituent to the ferrocene moiety, the Mössbauer quadrupole splitting (q.s.) value is seen to increase [11,12]. The opposite is observed with electron withdrawing groups [11–14]. Building on these findings enables understanding of the electronic interaction between the ferrocenyl iron and other metals [10,13].

2. Experimental

All reactions were carried out using dried and freshly distilled solvents. The starting materials were purchased from the Aldrich Chemical Company Ltd. ^{1}H-NMR

* Corresponding author. Tel.: +44-208-3318673; fax: +44-208-3318405.
E-mail address: sj29@gre.ac.uk (J. Silver).
[1] Present address: Department of Chemistry, Bedson Building, University of Newcastle upon Tyne, Newcasstle upon Tyne NE1 7RU, UK.

0022-328X/01/$ - see front matter
PII: S0022-328X(01)00925-1

spectra were recorded on a JEOL JNM-EX 270 FT-NMR system by Dr J. Warmsley. IR spectra were recorded on a Perkin–Elmer 1600 series FTIR spectrophotometer as Nujol mulls or KBr disks. Mössbauer spectra were recorded as described previously [14,15].

2.1. Preparation of 2-pyridyl hydrazone of ferrocene carbaldehyde (*1*), its metal complexes (*2–9*), and its protonated derivatives (*10–13*) (Table 1)

Preparation of the parent ligand [Fe(η^5-C_5H_5)(η^5-$C_{11}H_{10}N_3$)] (**1**) (referred to as complex **1** in Table 1) was carried out via the published procedure [16]. Metal complexes with general formula **1**MCl_2 were prepared as follows. Cadmium(II) chloride (0.09 g, 0.49 mmol) was dissolved in abs. EtOH over 24 h and mixed with **1** (0.15 g, 0.49 mmol). The solution changed to a deep red colour immediately and then after a few minutes became bright orange. The volume was reduced and the orange powder filtered off. This was recrystallised from abs. EtOH, washed with diethyl ether and dried under vacuum (**2**). Yield 0.14 g, 60%. Further metal complexes were prepared via an analogous method to that of **2**, where the procedures were carried out under anaerobic conditions. 1:1 molar ratios of the metal chloride to **1** were used giving the following yields for the derivatives of, copper(II) chloride (0.14 g, 67%) (**3**), zinc(II) chloride (0.47 g, 71%) (**4**), iron(II) chloride (0.55 g, 67%) (**5**), tin(II) chloride (0.33 g, 56%) (**6**) and palladium(II) chloride (0.17 g, 54%) (**7**). Further metal complexes with general formula [**1**$M(H_2O)_4$][PF_6]$_2$ were prepared as follows. Iron(II) chloride (0.2 g, 1.6 mmol) was dissolved in the minimum quantity of abs. EtOH and mixed with **1** (0.5 g, 1.6 mmol) in CH_2Cl_2 (40 cm^3) forming a deep red solution. Hexafluorophosphoric acid (0.5 cm^3, ca. 3 mmol) was added and the solution changed to a deep purple colour. The sample precipitated and was filtered off, dried and stored under nitrogen. Yield 0.73 g, 63% (**8**). The zinc complex was prepared by dissolving **7** (0.1 g, 2.2 mmol) in CH_2Cl_2 (30 cm^3) and hexafluorophosphoric acid (0.5 cm^3, ca. 3 mmol) was added again resulting in a deep purple coloration. A violet precipitate formed, was filtered off, washed in diethyl ether and dried under vacuum. Yield 0.9 g, 60% (**9**). Protonation of **1** was achieved by dissolving **1** in the minimum quantity of CH_2Cl_2 and adding in a 1:1 molar ratio HCl (**10**), HPF_6 (**11**), CH_3CO_2H (**12**) or CF_3CO_2H (**13**). Yields were between 55 and 65%. Elemental analysis for all samples is presented in Table 1.

2.2. Crystal and data collection details

A red plate-like crystal of **10** with dimensions of $0.20 \times 0.14 \times 0.06$ mm was mounted on a glass fibre. The chemical formula is $C_{16}H_{15}FeN_3 \cdot HCl$, unit cell parameters are $a = 16.250(8)$, $b = 11.585(3)$, $c = 16.515(8)$ Å, $\beta = 105.83(2)°$ with Mo–K_α radiation of 0.71073 Å. The crystal was found to be monoclinic with a non-standard space group setting of $P2_1/n$ and there are eight molecules in the unit cell. An Enraf–Nonius CAD4 diffractometer was used in the ω–2θ scan mode. 5243 data were collected and 2106 used with a cut-off criterion of $2\sigma(I)$. Weighted R-factors (wR) are based on F^2, conventional R-factors (R) are based on F, with F set to zero for negative F^2. The following weighting scheme was used, $w = 1/[\sigma^2(F_o^2) + (0.0696P)^2 + 0.0000P]$ where $P = (F_o^2 + 2F_c^2)/3$. A final R value of 0.05 and wR of 0.14 were obtained for 379 parameters. Refinement was against F^2 with hydrogen atoms placed geometrically.

Table 1
Microanalysis for samples **1–13**

Compound	Number	C (%)	H (%)	N (%)	Colour
1	**1**	62.9 (63.0)	5.0 (4.9)	13.8 (13.8)	Rust
1$CdCl_2$	**2**	39.2 (39.5)	3.1 (2.7)	8.3 (8.4)	Orange
1$CuCl_2$	**3**	43.8 (43.7)	3.6 (3.4)	9.3 (9.6)	Brown
1$ZnCl_2$	**4**	42.8 (43.5)	3.6 (3.4)	9.4 (9.5)	Orange
1$FeCl_2$	**5**	44.4 (43.9)	3.6 (3.4)	9.7 (9.4)	Red
1$SnCl_2$	**6**	36.8 (36.3)	3.0 (3.2)	7.9 (7.9)	Orange
1$PdCl_2$	**7**	39.1 (39.8)	2.7 (3.1)	8.6 (8.7)	Brown
[**1**$Fe(H_2O)_4$][PF_6]$_2$	**8**	26.4 (26.6)	3.3 (3.2)	5.4 (5.8)	Purple
[**1**$Zn(H_2O)_4$][PF_6]$_2$	**9**	25.7 (26.2)	2.9 (3.1)	5.2 (5.7)	Violet
1HCl	**10**	56.0 (56.2)	4.3 (4.7)	12.2 (12.3)	Ruby
1HPF_6	**11**	42.7 (42.6)	3.7 (3.5)	9.5 (9.3)	Ruby
1CH_3CO_2H	**12**	58.7 (59.2)	5.2 (4.8)	11.1 (11.5)	Rust
1CF_3CO_2H	**13**	50.9 (51.6)	3.9 (4.1)	10.1 (10.0)	Red

Experimental (calculated) values.

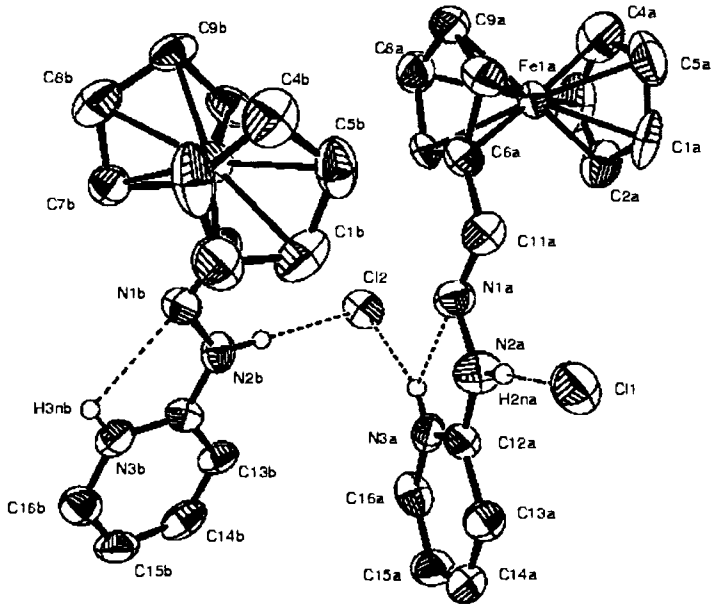

Fig. 1. Asymmetric unit and labelling scheme for the crystal structure of **10**.

3. Results and discussion

3.1. Crystal structure of *10*

Fig. 1 shows an ORTEP diagram of the asymmetric unit with the atom numbering scheme. The hydrochloride of **1** crystallises in the space group $P2_1/n$ with two different sets of **1**·HCl in the asymmetric unit. Hydrogen atoms were not found in the X-ray analysis and have been placed in trigonal positions on N(2) and N(3) of both cations. These cations are then found to be linked to the chloride ions by a zig–zag hydrogen-bonded chain. There are also intramolecular hydrogen bonds between N(1) and N(3) of both cations, so that the pyridinium hydrogen atoms, H(3n) show bifurcated hydrogen bonding to N(1) and to a chloride ion. These chains propagate in the [1 0 −1] direction along the n-glide plane, i.e. across the long diagonal of the *a*–*c* plane, perpendicular to the *b*-axis. The *n*-glide plane is an inherent property of the chain and the $Cl(1)^-$ anions lie almost in the plane.

Bond lengths and angles for the chain are shown in Tables 2 and 3, respectively. Angles at H of 180° imply singly hydrogen bonded hydrogen and angles at hydrogen of around 120° which sum to near 360° indicate bifurcated hydrogen bonds. Each chloride atom is bonded to two hydrogen atoms, one of which is singly hydrogen-bonded (N(2)–H(2n)···Cl(2)) and the other bifurcated (N(3)···Cl(2)···N(1)).

In each cation the pyridyl hydrazone fragment is coplanar with the cyclopentadienyl (Cp) rings indicating that there is conjugation throughout the cation which is in keeping with its Mössbauer spectroscopic

Table 2
Bond lengths for compound **10**

Bond length	Molecule A	Molecule B
C6–C11	1.456(9)	1.442(9)
C11–N1	1.283(8)	1.278(8)
N1–N2	1.397(8)	1.371(7)
N2–C12	1.343(8)	1.324(8)
Cl1–H2NA	2.257	2.257
N1A–H3NA	2.293	2.293
H3NA–Cl2	2.403	2.403
Cl2–H2NB	2.231	2.231
N1B–H3NB	2.339	2.339
H3NB–Cl1	2.380	2.380

Table 3
Bond angles for compound **10**

Bond angle	Molecule A	Molecule B
C7–C6–C11	125.9(7)	126.4(7)
C6–C11–N1	119.9(7)	122.1(7)
C11–N1–N2	115.1(6)	115.8(6)
N1–N2–C12	118.4(6)	119.9(6)
N2–C12–N3	118.7(7)	119.6(6)
H3NB–CL1–H2NA	92.7	92.7
Cl1–H2NA–N2A	176.6	176.6
H2NA–N2A–N1A	120.8	120.8
N2A–N1A–H3NA	78.5	78.5
N1A–H3NA–Cl2	102.0	102.0
H3NA–Cl2–H2NB	76.6	76.6
Cl2–H2NB–N2B	175.0	175.0
H2NB–N2B–N1B	120.1	120.1
N2B–N1B–H3NB	78.0	78.0
N1B–H3NB–CL1	108.5	108.5

Table 4
Mössbauer spectroscopic data for **1**–**13**

Sample	Number	T (K)	i.s. (mm s^{-1})	q.s. (mm s^{-1})	$\Gamma_{1/2}$ (mm s^{-1})
Ferrocene		80	0.52	2.37	0.14
1	**1**	80	0.50	2.29	0.15
	1	298	0.46	2.28	0.14
1$CdCl_2$	**2**	80	0.50	2.24	0.15
1$CuCl_2$	**3**	80	0.51	2.22	0.14
1$ZnCl_2$	**4**	80	0.53	2.23	0.13
1$FeCl_2$	**5**	80	0.54	2.24	0.12
			1.05	3.43	0.12
1$FeCl_2$	**5**	298	0.51	2.28	0.13
			1.01	3.28	0.13
1$SnCl_2$	**6**	80	0.50	2.25	0.13
			1.34 [a]	1.14 [a]	
1$PdCl_2$	**7**	80	0.50	2.23	0.18
[**1**$Fe(H_2O)_4$][PF_6]$_2$	**8**	80	0.50	2.08	0.15
			1.40	3.62	0.16
[**1**$Fe(H_2O)_4$][PF_6]$_2$	**8**	298	0.44	2.25	0.12
			1.28	3.43	0.14
[**1**$Zn(H_2O)_4$][PF_6]$_2$	**9**	80	0.49	2.08	0.13
1HCl	**10**	80	0.53	2.28	0.14
		298	0.46	2.28	0.11
1HPF_6	**11**	80	0.52	2.18	0.13
		298	0.46	2.26	0.11
1CH_3CO_2H	**12**	80	0.53	2.30	0.13
		298	0.44	2.30	0.12
1CF_3CO_2H	**13**	80	0.54	2.29	0.11
		298	0.46	2.23	0.11

[a] ^{119}Sn data relative to α-tin, ^{57}Fe i.s. relative to natural iron. All parameters are quoted with an error of ± 0.01 mm s^{-1}.

data (see below). This is also in keeping with the previously published [16] crystal structure of **1** which has planar units but in which the pyridyl group has the opposite configuration, being rotated 180° about the N(2)–C(12) bond so that the pyridyl nitrogen N(3) is *trans* to N(1). The protonated pyridyl hydrazone fragment of **10** comprises the most interesting component of the crystal structure as its configuration exhibits the potential bidentate binding site for an acceptor atom, i.e. replacing the proton, H(3n), so that N(1) and N(3) become the donors of a chelate ring. The geometrical properties in the cations labelled a and b are very similar and both are planar (apart from the Fe and C(1) to C(5) rings). A comparison of this structure with that of **1** indicates some differences in the bond lengths. In **1** the N(2)–C(12) bond length is longer at 1.377(4) Å and shows less partial nitrogen lone pair delocalization as observed for the equivalent bonds in **10**. Bonds to N(1) are lengthened in **10** as opposed to **1** which is expected since N(1) forms part of the hydrogen bonding network of the structure.

3.2. Mössbauer spectroscopic data

Detailed analysis has been carried out using ^{57}Fe Mössbauer spectroscopy to probe the iron environments in all the complexes. Where appropriate ^{119}Sn Mössbauer spectroscopy was also used. Mössbauer spectroscopic data are reported in Table 4. Complexes **5** and **8** were found to be air sensitive (see Figs. 2 and 3 for a schematic representation of **5** and **8**, respectively).

Assessment of the 80 K data for the ligand (**1**) shows that relative to ferrocene the Schiff base is withdrawing electrons from the Cp ring, indicated by the reduction of the q.s. It is noted that the isomer shift (i.s.) is relatively invariant over all the measurements for the ferrocenyl iron site. In both compounds **1** and **10** the

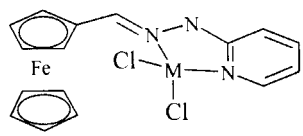

Fig. 2. Schematic representation of **5**.

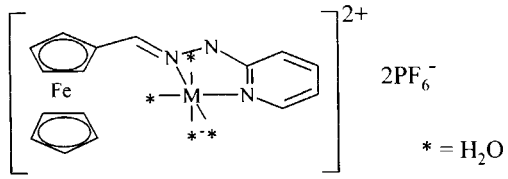

Fig. 3. Schematic representation of **8**.

Table 5
Mössbauer spectroscopic data for $[FeX_4]^{2-}$ anions [20] [a]

Compound	i.s. (mm s^{-1})	q.s. (mm s^{-1})	T (K)
$[NMe_4]_2[FeCl_4]$	1.05	3.27	4.2
	1.01	2.61	77
	0.91	0.72	293
$[NEt_4]_2[FeCl_4]$	1.01	3.21	4.2
	1.00	2.68	77
	0.99	1.16	293
$[(PQ)_2][FeCl_4]$ [b]	1.01	3.02	4.2
	1.00	2.99	77
	0.88	2.51	293
$[NEt_4]_2[FeBr_4]$	1.12	3.23	4.2
	1.02	2.29	77
	0.88	0.52	293
$[NMe_4]_2[Fe(NCS)_4]$	0.97	2.83	4.2
	0.97	2.10	77
$[(Cat)_2][Fe(NCSe)_4]$ [c]	1.04	2.73	4.2
	0.99	2.69	77
	0.86	2.19	195

[a] Mössbauer parameters quoted ± 0.05 mm s^{-1}.
[b] PQ = *N*,*N*′-dimethyl-4,4′-dipyridyl.
[c] Cat = α,α′-bis(triphenylphosphonium)*p*-xylene.

q.s. value is the same, showing that the electron withdrawal by the pyridyl side chain is identical indicating that: (1) the configuration of the side chain does not affect the q.s. and (2) the hydrogen bonding in **10** does not affect the q.s. relative to the parent, hence it is not very electron withdrawing from the pyridyl ring, rather surprising as it might be expected that protonation would increase the electron-withdrawing property.

When **1** is complexed to the metal(II) chlorides (**2**–**7**) the q.s. is seen to reduce even further showing that in contrast to hydrogen bonding the metals pull electron density out of the Cp ring.

^{119}Sn Mössbauer data for **6** probe the coordinated metal site. Classically ^{119}Sn Mössbauer spectroscopy has not been as informative as that of ^{57}Fe for indicating coordination due to the lack of comparative data available. The i.s. value identifies that Sn(II) is present. From a literature search there are some data that can be usefully applied for elucidating the ligand arrangement around the Sn(II) centre for compound **6**, however the quantity of data is very sparse so assignment is tentative. Mössbauer spectroscopic data for [$SnCl_2$(2,2′-bipyridine)] gives i.s. = 1.43 mm s^{-1} and q.s. = 1.16 mm s^{-1} and for [$SnCl_2$(1,10-phenanthroline)] gives i.s. = 1.46 mm s^{-1} and q.s. = 1.07 mm s^{-1} (i.s. relative to SnO_2) [17]. This indicates Sn(II) complexation and also the q.s. values are very similar to that of the tin complex **6** which gives an indication that the ligand spatial arrangement should also be similar. Sn(II) crystal structures have been elucidated of the general type $Sn(N)_2Cl_2$. These include the 2,2′-bipyridine and 1,10-phenanthroline compounds where $(N)_2$ is bidentate [18] and the 1-vinylimidazole and 1-benzylimidazole compounds where two monodentate ligands are present [19]. In the latter two structures the chlorides are *trans* to each other with angles nearer 180° than 90° [19]. In the bidentate ligand structures the chlorides are *cis* with angles very close to 90° [18]. Both types of complex are in a distorted pseudo-five coordination giving a distorted trigonal bipyramidal geometry, where the Sn(II) non-bonding lone-pair occupy the fifth coordination site. It is therefore likely that compound **6** contains *cis* chlorides. Moreover the bite angle of the Sn(II) to the nitrogen atoms in **6** will be similar to that of the other compounds **2**–**5**.

Complex **5** contains a second coordinated iron atom that offers additional information on the bonding of the molecule to the ^{57}Fe Mössbauer spectroscopic probe. The parameters for this site (Table 4) are i.s. 1.05 mm s^{-1} and q.s. 3.43 mm s^{-1}, indicative of high spin iron(II). Compound **5** has similar i.s. values to those of known iron(II) tetrahedral sites (see Table 5) [20] and thus fits a distorted tetrahedral coordination. In $[FeCl_4]^{2-}$ anions the i.s. and the q.s. reduce with increasing temperature (Table 5), the latter being due to an increase in symmetry of the iron. The q.s. values of the $[Fe(NR)_4]^{2-}$ anions (Table 5) exhibit little temperature dependence just as the species in compound **5**. Hence assignment of a distorted tetrahedral electronic environment to the coordinated iron of complex **5** is made.

Compound **8** also contains an Fe(II) cation coordinated to **1**, its i.s. value is higher than that of compound **5** at both temperatures studied, and is indicative of high spin Fe(II) in a distorted octahedral environment similar to that of $FeCl_2(H_2O)_4$. In the latter compound the Cl atoms are *cis* and we would expect a similar geometry with **1** replacing the two Cl^- ligands. The q.s. value for the inorganic Fe(II) site in **8** is similar to $[Fe(H_2O)_6]^{2+}$ species [21,22], and is larger than those of $FeCl_2(H_2O)_4$; they manifest similar temperature dependence to the former compound. Thus we assign a distorted six coordinated electronic site to the Fe(II) in complex **8**, in this case unlike in compound **5** the positive charge on the Fe(II) is not compensated in its first coordination sphere. This means there is a 2+ charge close to the iron in the ferrocenyl site in compound **8**. Similarly for the Zn(II) (compound **9**) equivalent compound there will be a Zn^{2+} close to the ferrocenyl iron(II). The 80 K q.s. values for the ferrocenyl iron(II) sites in compounds **8** and **9** are identical (Table 4) and the value of 2.08 mm s^{-1} is particularly small. It has previously been shown that q.s. values as small as this indicated that substantial electron density has been removed from the ferrocenyl iron [11–13]. The question that remains is 'how is this electron density withdrawn from the iron of the ferrocene?' To answer this the rest of the data in Table 4 must be considered.

Compounds **2**–**7** are all of the type **1**MCl_2, and all manifest a q.s. value of 2.22 to 2.25 mm s^{-1} for the ferrocenyl iron sites. Compounds **2**–**5** are all expected to have the M atoms in similar distorted tetrahedral sites. All are expected to have similar electron withdrawal power from **1** and offer similar ligating geometry. This would be in keeping with the q.s. values for the ferrocenyl iron atoms in compounds **2**–**5** (all 2.23(1) mm s^{-1} at 80 K). Compound **6** would be expected to contain the Sn(II) atom in a trigonal bipyramidal site and hence exert a similar ligating geometry to the ligand **1**. However the Sn(II) cation would be expected to be more electron rich due to the presence of its two non-bonding valence electrons. Thus it would need less electron density from **1**. The ferrocenyl iron in compound **6** has a q.s. of 2.25 mm s^{-1}, which although only slightly larger than those of compounds **2**–**5** does indicate less electron withdrawal. Compound **7** contains Pd(II) and this might be expected to prefer square planar coordination [2]. However, from the q.s. of the iron in its ferrocenyl moiety its electron withdrawal through its coordination to **1** makes similar demands to those in compounds **2**–**5**.

In all the compounds **2**–**7** the M^{2+} cations are charge compensated by the $2Cl^-$ anions in their first coordination sphere. Thus the iron atoms in the ferrocenyl moieties of their ligand **1** are not fully exposed to the charge on the M^{2+} ions. This can be seen from models of compounds **2**–**7** based on the structures of compounds **1** [16] and **10**. These indicate that the Cl^- ions are above and below the level of the plane of pyridyl hydrazone, placing a Cl^- ion between the M^{2+} and the iron of the ferrocenyl moiety. This is not the case for compounds **8** and **9**, here only water molecules can come between the M^{2+} and the ferrocenyl iron atom. The latter atom therefore is exposed to the electric field of the M^{2+} ions, and this is the obvious cause of the low q.s. values of 2.08 mm s^{-1} (0.14 mm s^{-1} smaller than those of compounds **2**–**7**). It should be noted that such a small q.s. value has not previously been recorded for a singly substituted ferrocenyl moiety [23].

As electric field effects would be expected to fall off with $1/r^2$ then to experience field effects from external M^{2+} ions it would be necessary to bring the M^{2+} to within 5 Å of the iron atom of the ferrocene. Such effects would be expected to change the oxidation potential of the ferrocenyl moiety as q.s. values were shown to be related to oxidation potentials [24]. However at 6 Å the field would be almost twice as small as at 5 Å and thus be expected to affect the ferrocenyl much less [25]. Other evidence in support of this is found in Fig. 3 of Ref. [25a], for protonated amines, where the Fe–N distance is large, the change in the oxidation potential of the ferrocenyl iron is small.

In their Fig. 3, Beer et al. [25] present a plot of the inverse Fe–N distances in four ferrocene amines against the difference of the redox couples of ligands in their free and protonated forms. If the cationic charge is assumed to lie on the amine nitrogen in the protonated forms, the least change of oxidation potential (0.1 V) is found with the longest Fe–N distance ($\sim$5.50 Å). Extrapolating the distance in their Fig. 3 to zero change gives an Fe–N distance of $\sim$7.8 Å. In compound **10** the $Fe–N_{protonated}$ distances are 6.249 and 6.064 Å suggesting $E_2 - E_1$ values of approximately 70 mV, which is a relatively small change, and hence it is not surprising that the proton had no effect on the ferrocenyl q.s. value.

The q.s. of 2.08 mm s^{-1} for compounds **8** and **9** could be included on a plot of q.s. against quarter wave potentials [24,26,27] that we previously presented in Ref. [24]. If this is done a change in the quarter wave potential relative to ferrocene of around 0.900 mV is expected. This is a large change and very comparable to those reported for other ferrocenyl ligands where a cation is in very close proximity to the ferrocenyl iron [25]. This again provides evidence that the very low q.s. values of 2.08 mm s^{-1} for compounds **8** and **9** arise from a direct effect of the M^{2+} charge.

It should be noted that among the other acid salts of **1** only the HPF_6 salt (compound **11**) and the acetate (at 298 K) (compound **13**) show any significant lowering of the q.s. values relative to compound **1**.

A major difference in the acids used to protonate the ligand is the bulk of the anion. The largest is $[PF_6]^-$, which may not approach the ligand as closely as the smaller acid molecules such as the HCl in **10**. If this is correct it would explain the larger effect of the proton on the q.s. value of **11**. The temperature dependence of the q.s. in compounds **11** and **13** could be attributed to movement in the anionic acid counter-ions within the structure (due to temperature dependent rearrangement).

The 298 K data for compound **8** show the largest change in the ferrocenyl i.s. at 0.44 mm s^{-1} and the q.s. increases back up to 2.25 mm s^{-1}. The second site also manifests some temperature dependence with the i.s. and q.s. both reducing with an increase in temperature. This indicates that electron density withdrawal effects the q.s. by 0.03 mm s^{-1} via the conjugation effect in **8** and **9** and 0.17 mm s^{-1} via a charge effect as seen for **8**. The latter is lost at room temperature possibly by movement of the $[PF_6]^-$ anions as suggested above for the protonated salts where the ligand remains in what must be a planar conjugated pathway. In this case the $[PF_6]^-$ may hydrogen bond very strongly to the water molecules

bound to the M_2^+ cations. This would effectively either remove the protons leaving two hydroxyl ions bound or by each $[PF_6]^-$ ion hydrogen bonding to several protons across two or more water molecules, effectively leaving the oxygen atoms of the water molecules each partially negatively charged. In either case the resulting negative charges would shield the ferrocenyl iron from the M^{2+} charge and hence the q.s. rises to 2.25 mm s^{-1} and the environment is then comparable to those in compounds **2**–**6**.

Further evidence in support of such a change arises from the relative intensities of the iron sites. In **5** the two quadrupole doublets have equal intensities at both temperatures. In **8** the sites are equal at 80 K but not at 298 K, the ferrocenyl iron site being much reduced in intensity with a ratio of only 1:9 for the inorganic Fe(II) site. This shows that the Fe^{2+} site in **8** is held, at 298 K, in a much more rigid state than that of the iron atom in the ferrocenyl site of **8** or in the chloride coordinated iron site of **5** and would be in keeping with multi-hydrogen bonding to large $[PF_6]^-$ anions.

Finally it should be noted that only compounds **8** and **9** are purple. We have previously seen such dark colours only with protonation of the ferrocene itself [28]. This is further evidence for a field effect.

4. Conclusions

It has been shown that for a ferrocenyl compound when unshielded charge is close to the ferrocenyl iron atom the q.s. values are small. This is interpreted as a change in the electric field at the ferrocenyl iron due to the presence of the charge.

Mössbauer spectroscopy has also been used to identify the spin state and coordination of metals in ferrocenyl-pyridyl-imine ligand metal chloride complexes in the absence of crystal structure data. A route for electron delocalisation is proposed based upon the Mössbauer spectroscopic data.

Complex **5** has high spin tetrahedral iron(II) coordinated by two chloride ions and two nitrogen atoms of ligand **1**. Complex **8** also has high spin iron(II) but with octahedral coordination.

5. Supplementary material

Crystallographic data for the structural analysis have been deposited with the Cambridge Crystallographic Data Centre, CCDC no. 154800 for compound **10**. Copies of this information may be obtained free of charge from The Director, CCDC, 12 Union Road, Cambridge CB2 1EZ UK (Fax: +44-1223-336033; e-mail: deposit@ccdc.cam.ac.uk or www: http://www.ccdc.cam.ac.uk).

Acknowledgements

J.S. thanks the EPSRC and the Nitrogen Fixation Laboratory (BBSRC) for CASE awards for E.S. and G.R.F.

References

[1] P.D. Beer, J.E. Nation, S.W.L. McWhinnie, M.E. Harman, M.B. Hursthouse, M.I. Ogden, A.H. White, J. Chem. Soc. Dalton Trans. (1991) 2485.
[2] A. Houlton, S.K. Ibrahim, J.R. Dilworth, J. Silver, J. Chem. Soc. Dalton Trans. (1990) 2485.
[3] M.L.H. Green, S.R. Marder, M.E. Thompson, J.A. Bandy, D. Bloor, P.V. Kolinsky, R.J. Jones, Nature (Lond.) 330 (1987) 360.
[4] B.J. Coe, C.J. Jones, J.A. McCleverty, D. Bloor, P.V. Kolinsky, R.J. Jones, J. Chem. Soc. Chem. Commun. (1989) 1485.
[5] S. Ghosal, M. Samoc, P.N. Prasad, J.J. Tufariello, J. Phys. Chem. 94 (1990) 2847.
[6] G. Doisneau, G. Balavoine, T. Fillebeen-Kahn, J.-C. Clinet, J. Delaire, I. Ledoux, R. Loucif, G. Puccetti, J. Organomet. Chem. 421 (1991) 299.
[7] J.C. Medina, I. Gay, Z. Chen, L. Echegoyen, G.W. Gokel, J. Am. Chem. Soc. 113 (1991) 365.
[8] J.S. Miller, A.J. Epstein, W.M. Reiff, Chem. Rev. 88 (1988) 201.
[9] A. Houlton, J.R. Miller, J. Silver, N. Jasim, M.T. Ahmet, Inorg. Chim. Acta 205 (1993) 67.
[10] A. Houlton, J.R. Dilworth, R. Roberts, J. Silver, Polyhedron 22 (1990) 2751.
[11] A. Houlton, N. Jasim, R.M.G. Roberts, J. Silver, D. Cunningham, P. McArdle, T. Higgins, J. Chem. Soc. Dalton Trans. (1992) 2235.
[12] R. Bosque, M. Font-Bardía, C. López, J. Sales, J. Silver, X. Solans, J. Chem. Soc. Dalton Trans. (1994) 747.
[13] D.J. Evans, A. Hills, D.L. Hughes, G.J. Leigh, A. Houlton, J. Silver, J. Chem. Soc. Dalton Trans. (1990) 2735.
[14] G.A. Heath, R.L. Martin, I.M. Stewart, Aust. J. Chem. 22 (1969) 83.
[15] M.Y. Hamed, R.C. Hider, J. Silver, Inorg. Chim. Acta 66 (1982) 13.
[16] A. Houlton, M.T. Ahmet, J.R. Miller, J. Silver, E. Slade, Acta Crystallogr. Sect. C 49 (1993) 682.
[17] N.N. Greenwood, A. Timnick, J. Chem. Soc. A (1971) 676.
[18] S.J. Archer, K.R. Koch, S. Schmidt, Inorg. Chim. Acta 126 (1987) 209.
[19] S.V. Vasnin, J. Cetrullo, R.A. Geanangel, I. Bernal, Inorg. Chem. 29 (1990) 885.
[20] P.R. Edwards, C.E. Johnson, R.J.P. Williams, J. Chem. Phys. 47 (1967) 2074.
[21] B.Y. Enwiya, J. Silver, I.E.G. Morrison, J. Chem. Soc. Dalton Trans. (1982) 2231.
[22] R.C. Hider, A.R. Mohd-Nor, J. Silver, I.E.G. Morrison, L.V.C. Rees, J. Chem. Soc. Dalton Trans. (1981) 609.
[23] J. Silver, in: M. Gielen, R. Willem, B. Wrackmeyer (Eds.), Solid State Organometallic Chemistry: Methods and Applications, Wiley, 1999, p. 279.
[24] R.M.G. Roberts, J. Silver, J. Organomet. Chem. 263 (1984) 235.
[25] (a) P.D. Beer, P.A. Gale, G.Z. Chen, J. Chem. Soc. Dalton Trans. (1999) 1897;
(b) H. Plenio, R. Diodone, J. Organomet. Chem. 492 (1995) 73;
(c) H. Plenio, R. Diodone, Inorg. Chem. 34 (1995) 3964.
[26] W.F. Little, C.N. Reilley, J.D. Johnson, K.N. Lynn, A.P. Saunders, J. Am. Chem. Soc. 86 (1964) 1376.
[27] W.F. Little, C.N. Reilley, J.D. Johnson, A.P. Saunders, J. Am. Chem. Soc. 86 (1964) 1382.
[28] J. Silver, R.M.G. Roberts (1987), unpublished results.